NeuroImage: Clinical 34 (2022) 103010

Contents lists available at ScienceDirect

NeuroImage: Clinical

journal homepage: www.elsevier.com/locate/ynicl

A multi-regression approach to improve optical coherence tomography diagnostic accuracy in multiple sclerosis patients without previous optic neuritis

Jacqueline Chua [a,b,c], Mihai Bostan [d,e], Chi Li [a,c], Yin Ci Sim [a,c], Inna Bujor [d], Damon Wong [a,c,f], Bingyao Tan [a,c,f], Xinwen Yao [a,c,f], Florian Schwarzhans [g,h], Gerhard Garhöfer [h], Georg Fischer [g], Clemens Vass [i], Cristina Tiu [d,j], Ruxandra Pirvulescu [d,k], Alina Popa-Cherecheanu [d,k,*], Leopold Schmetterer [a,b,c,f,h,l,m,*]

[a] Singapore Eye Research Institute, Singapore National Eye Centre, Singapore
[b] Ophthalmology and Visual Sciences Academic Clinical Program, Duke-NUS Medical School, National University of Singapore, Singapore
[c] SERI-NTU Advanced Ocular Engineering (STANCE), Singapore, Singapore
[d] Carol Davila University of Medicine and Pharmacy, Bucharest, Romania
[e] Ophthalmology Emergency Hospital, Bucharest, Romania
[f] School of Chemical and Biological Engineering, Nanyang Technological University, Singapore
[g] Center for Medical Statistics Informatics and Intelligent Systems, Section for Medical Information Management, Medical University Vienna, Vienna, Austria
[h] Department of Clinical Pharmacology, Medical University Vienna, Vienna, Austria
[i] Department of Ophthalmology and Optometry, Medical University Vienna, Vienna, Austria
[j] Emergency University Hospital, Department of Neurology, Bucharest, Romania
[k] Emergency University Hospital, Department of Ophthalmology, Bucharest, Romania
[l] Center for Medical Physics and Biomedical Engineering, Medical University Vienna, Vienna, Austria
[m] Institute of Molecular and Clinical Ophthalmology, Basel, Switzerland

ARTICLE INFO

Keywords:
Relapsing-remitting multiple sclerosis
Optical coherence tomography
Peripapillary retinal nerve fiber layer
Macular ganglion cell and inner plexiform layer
Macular ganglion cell complex

ABSTRACT

Background: Optical coherence tomography (OCT) is a retinal imaging system that may improve the diagnosis of multiple sclerosis (MS) persons, but the evidence is currently equivocal. To assess whether compensating the peripapillary retinal nerve fiber layer (pRNFL) thickness for ocular anatomical features as well as the combination with macular layers can improve the capability of OCT in differentiating non-optic neuritis eyes of relapsing-remitting MS patients from healthy controls.

Methods: 74 MS participants (n = 129 eyes) and 84 age- and sex-matched healthy controls (n = 149 eyes) were enrolled. Macular ganglion cell complex (mGCC) thickness was extracted and pRNFL measurement was compensated for ocular anatomical factors. Thickness measurements and their corresponding areas under the receiver operating characteristic curves (AUCs) were compared between groups.

Results: Participants with MS showed significantly thinner mGCC, measured and compensated pRNFL ($p \leq 0.026$). Compensated pRNFL achieved better performance than measured pRNFL for MS differentiation (AUC, 0.75 vs 0.80; $p = 0.020$). Combining macular and compensated pRNFL parameters provided the best discrimination of MS (AUC = 0.85 vs 0.75; $p < 0.001$), translating to an average improvement in sensitivity of 24 percent for differentiation of MS individuals.

Conclusion: The capability of OCT in MS differentiation is made more robust by accounting OCT scans for individual anatomical differences and incorporating information from both optic disc and macular regions, representing markers of axonal damage and neuronal injury, respectively.

Abbreviations: AUC, areas under the receiver operating characteristic curve; GCL, ganglion cell layer; INL, inner nuclear layer; IPL, inner plexiform layer; IOP, intraocular pressure; MS, multiple sclerosis; OCT, optical coherence tomography; RNFL, retinal nerve fibre layer.

* Corresponding authors at: 20 College Road, The Academia, Level 6, Discovery Tower, Singapore 169856, Singapore (L. Schmetterer). Carol Davila University of Medicine and Pharmacy, Bucharest, Romania (A. Popa-Cherecheanu).

E-mail addresses: alina_cherecheanu@yahoo.com (A. Popa-Cherecheanu), leopold.schmetterer@meduniwien.ac.at, leopold.schmetterer@seri.com.sg (L. Schmetterer).

https://doi.org/10.1016/j.nicl.2022.103010
Received 24 August 2021; Received in revised form 12 April 2022; Accepted 12 April 2022
Available online 16 April 2022

1. Introduction

Multiple sclerosis (MS) is a chronic disabling disease of the central nervous system that typically affects young people at their prime (McGinley et al., 2021). Because the diagnosis of MS remains challenging, there is a substantial interest to utilize optical coherence tomography (OCT) as a complementary diagnostic tool (Thompson et al., 2018). The motivation for including OCT in the diagnostic routine of MS patients stems from the observations of pRNFL and macular ganglion cell and inner plexiform layer (mGCIPL) thinning in the eyes of MS patients even in those without a history of optic neuritis, suggesting that the retinal axonal injury may be independent of acute optic nerve inflammation (Petzold et al., 2017).

Significant thinning of mGCIPL in non-optic neuritis eyes of MS patients is now firmly established (Petzold et al., 2017). However, previous MS studies showed pRNFL thickness diagnostic sensitivity to be significantly variable, especially when considering non-optic neuritis eyes (Albrecht et al., 2012; Behbehani et al., 2016; Gonzalez-Lopez et al., 2014; Knier et al., 2016; Oberwahrenbrock et al., 2013; Para-Prieto et al., 2021; Parisi et al., 1999; Syc et al., 2012). A previous study reported the capacity of pRNFL thickness in assessing MS was lower as compared to mGCIPL (Gonzalez-Lopez et al., 2014). The poorer accuracy of pRNFL may be related to the wide variability of pRNFL. Indeed, interindividual variability is often wider for pRNFL parameter compared to mGCIPL (Para-Prieto et al., 2021). A broad range of pRNFL measurements creates difficulties in establishing an absolute diagnostic cutoff with good sensitivity and specificity. Most of these studies have adjusted for age when comparing the pRNFL measurements between MS and controls but important ocular anatomical features (e.g., retinal vessel profile (Choi et al., 2014; Hood et al., 2008; Resch et al., 2016)), have been considered. Additionally, a recent *meta*-analysis has recommended that OCT scans from two different ocular regions (optic disc and macular area) be routinely included in MS diagnosis and research (Petzold et al., 2017). It remains unclear the incremental diagnostic values of having both OCT scans for MS differentiation as compared to individual scans.

We recently developed a regression-based model (multi-regression) from healthy Caucasians to compensate pRNFL thickness for ocular anatomical features (Chua et al., 2020a; Pereira et al., 2015). Our newly compensated pRNFL thickness demonstrated a smaller interindividual variability and may improve MS differentiation. In this study, we determine if the diagnostic ability of OCT to differentiate MS individuals from controls can be further improved by 1) compensating the pRNFL thickness for individual differences and 2) combining pRNFL thickness with macular information.

2. Methods

This study was conducted by the principles of the Declaration of Helsinki and approved by the Emergency University Hospital Bucharest Institutional Review Board. Written informed consent from the participants was obtained after providing a detailed explanation of the study. This study was designed as a prospective, cross-sectional case-control study, enrolling participants ages 18 years of age or older, and was conducted from August 2020 to January 2021.

MS diagnosis was confirmed by the treating neurologist based on the 2017 McDonald criteria (Thompson et al., 2018). Expanded Disability Status Scale (EDSS) evaluations were performed by a neurologist where the score ranges from 0 to 10 in 0.5-unit increments representing higher levels of disability (Kurtzke, 1983). Only participants with relapsing-remitting MS who were on MS treatment were included. MS participants with a history of optic neuritis in either eye and/or patients with either primary progressive MS or secondary progressive MS were excluded from the study by the patient's treating neurologist. Medical records were screened to determine the disease-modifying therapies use, disease duration, numbers of relapsing episodes, and presence of optic neuritis. Patients were excluded if they had acute or past optic neuritis. Controls also attended the same clinic but were free of any neurological and/or any other relevant medical condition. Participants were excluded from the study if they had received ocular surgery, ocular diseases such as glaucoma, age-related macular degeneration and/or sight-threatening ocular disease. The presence of glaucomatous optic neuropathy was defined as loss of neuroretinal rim with a vertical cup: disc ratio of > 0.7 or an inter-eye asymmetry of >0.2 and/or notching attributable to glaucoma. All participants received a comprehensive ophthalmological examination, including visual acuity using the ETDRS acuity charts, refractive error, intraocular pressure, axial length measurements, slit lamp biomicroscopy, and fundoscopy.

2.1. Optical coherence tomography

OCT scans were performed using the Cirrus spectral domain-OCT (Carl Zeiss Meditec, Inc, Dublin, CA, USA) which was operated from a single site by one trained technician. OCT scans were obtained on the same day with other measurements. Pupils were not dilated prior to OCT imaging instead room lighting was dimmed to achieve maximal pupil dilation. Two different volumetric scan protocols were acquired one centered on the macula (512 A-scans $\times$ 128B-scans; 6 $\times$ 6 mm) and the other centered on the optic disc (200 A-scans $\times$ 200B-scans; 6 $\times$ 6 mm) (Chua et al., 2020a). Each OCT scan was evaluated according to APOSTEL recommendations and the OSCAR-IB protocol for quality control (Aytulun et al., 2021; Tewarie et al., 2012). One trained grader masked to the participant's characteristics reviewed the quality of OCT datasets. Eyes with poor quality images (signal strength <6 and/or movement artifacts causing off-centration, breakages, inconsistent signal intensity across the scan (poorly or unevenly illuminated scans), algorithm failures resulting in segmentation errors, and/or eyes with ocular pathology and missing variables were excluded (Chua et al., 2020b).

2.2. Individual retinal layer thickness analysis

Segmentation of the macular (1) RNFL, (2) ganglion cell layer (GCL), and (3) inner plexiform layer (IPL) was performed utilizing the Iowa Reference Algorithm (Retinal Image Analysis Lab, Iowa Institute for Biomedical Imaging, Iowa City, IA, USA) (Fig. 1**A**). All analyses were corrected for ocular magnification. Average retinal thickness was calculated within an annulus, centered on the fovea with an inner diameter of 1 mm and an outer diameter of 2.5 mm. We computed the macular ganglion cell complex (mGCC, combining RNFL + GCL + IPL) and the mGCIPL (GCL + IPL).

In this study, we used the Iowa Reference Algorithm to extract the retinal layers instead of the automatic segmentation algorithm provided by the Cirrus device. There are two reasons for using a customized program. First, it will allow us to rescale the OCT scans whereas the Cirrus device does not perform such rescaling. Measurements performed with OCT have inherent errors when the scale of the retinal image is not corrected for the axial length of each eye (Savini et al., 2012). Second, it will allow us to extract the individual macular layers and study the contribution of each macular layer to MS detection whereas the Cirrus device only provides the combined GCIPL layer measurements.

The Littman and modified Bennett formulas were used to calculate true image size (Higashide et al., 2016). Briefly, the relationship between the measured OCT image diameter (s) and the true diameter of the fundus ($s_{\text{corrected}}$) is expressed as $s_{\text{corrected}} = p \times q \times s$ (Bennett et al., 1994), where $s_{\text{corrected}}$ is the actual fundus dimension, s is the scanning size of the protocol obtained using OCT, p is the magnification factor for the camera of the imaging system, and q is the factor related to the eye ($q = 0.01306 \times [\text{axial length} - 1.82]$). For the Cirrus system, the value of the magnification factor (p) is 3.382 (Leung et al., 2007). According to the formula, $s_{\text{corrected}}$ can be calculated based on scan size ($s = 2.5$ mm) area as: $s_{\text{corrected}} = 3.382 \times 0.01306 \times (\text{axial length} - 1.82) \times 2.5$.

2.3. Compensation of peripapillary retinal nerve fiber layer thickness

We compensated the peripapillary retinal nerve fiber layer pRNFL thickness for numerous factors (optic disc [ratio, orientation, and area], fovea [distance and angle], retinal vessel density, refractive error, and age, using a previously described multivariate linear regression-based model (Pereira et al., 2015). Optic disc ratio refers to the quotient between major and minor axis, and orientation refers to the angle between the horizontal axis and the major axis of the optic disc. Briefly, pRNFL thickness measurements were extracted from the optic disc OCT scans using the Cirrus Review Software (software version 11.0.0.29946). OCT images were then imported into MATLAB (MathWorks Inc., R2018b, Natick, MA) to extract the relevant factors. (Fig. 1**B**). We generated the compensated pRNFL thickness and obtained the averaged measurements within the 3.4 mm ring around the optic disc center.

Supplementary Figure 1 shows the association of retinal blood vessels and the pRNFL. Our current compensation model delineates the vessels with appropriate angles and summed up the thickness values of all measured vessels within each sector (Pereira et al., 2015; Pereira et al., 2014). The resulting set of data was convolved with a Gaussian-shaped function, to generate a circumpapillary retinal vessel density profile.

2.4. Statistical analyses

Both eyes of each participant were included in this study according to the eligibility criteria described. Primary outcomes were the capability of retinal thickness measurements for MS differentiation. Shapiro-Wilk test was used to assess the normality of the distribution of the continuous variables. To compare the characteristics between MS and controls, the Kruskal-Wallis test was performed for non-normally distributed continuous variables, an independent *t*-test was performed for normally distributed continuous variables, and chi-square or Fisher's exact tests were performed for categorical variables. Mean thickness of different layers was compared between the groups using a multivariate linear regression model with generalized estimating equations (GEE), adjusted for potential confounders such as age, sex, systemic hypertension, IOP, and signal strength and inter-eye correlation. We assessed the performance of OCT measurements in discriminating MS from controls using the receiver operating characteristic (ROC) curve. Logistic regression model including several retinal layers as predictors was built. For example, to build up a model for mGCC, we included three layers: RNFL + GCL + IPL. Each retinal parameter was tested one at a time in the logistic regression models. This meant that the mGCC and mGCIPL are not entered in the same model. To avoid α error accumulation due to multiple testing between macular layers (mGCIPL with mGCC) and peripapillary parameters (measured pRNFL thickness and compensated pRNFL thickness), we used a conservative Bonferroni correction and considered results statistically significant at the level $\alpha = 0.05/2 = 0.025$. For all other analyses, a P value < 0.05 was considered statistically significant. Because therapy can modulate RNFL changes (Button et al., 2017), we determined the pRNFL thickness by medication classes. From these coefficients of the outcome, a predicted probability of the outcome for each observation was calculated which was then used to estimate the area under the curve (AUC) of the model (Cleves, 2002). Clustered bootstrapping was used for inference to account for correlation amongst observations (eyes) for the same individual. The sensitivity at 80% specificity was also calculated. The AUCs for OCT measurements were compared using the DeLong test (Hanley and McNeil, 1983). Data analysis was performed with Stata version 16.1 (StataCorp LLC, College Station, TX).

3. Results

Of the 105 normal controls (n = 208 eyes) and 83 MS participants (n = 166 eyes) who underwent OCT imaging, we excluded 59 eyes from controls and 37 eyes from MS participants for poor quality OCT scans, leaving 84 controls (n = 149 eyes) and 74 MS participants (n = 129 eyes) for analysis (Supplementary Figure 2).

Time from diagnosis of MS ranged from 1 to 37 years with a median of 8 years. We did a subgroup analysis by patient disease duration, where we performed a median split of the subjects into short disease duration (1–8 years; n = 40) and long disease duration (9–37 years; n = 34). MS participants with longer disease duration reported fewer episodes of neurological episodes (5.8 ± 6.1 vs 2.4 ± 1.1; $p = 0.001$) with worse EDSS scores (2.6 ± 0.8 vs 2.2 ± 0.7; $p = 0.036$) than recently diagnosed MS individuals. The mean ± standard deviation (SD) age of participants was 40 ± 11 years and 65% were female (Table 1). Apart from higher IOP amongst MS participants as compared to controls ($p < 0.001$), there were no differences between groups in terms of age, sex, diabetes, hypertension, visual acuity, signal strength, optic disc, and foveal features as well as the refractive error ($p = 0.087$).

After adjusting for age, sex, systemic hypertension, IOP, signal strength, and inter-eye correlation, pRNFL thickness was significantly thinner in MS participants than in normal controls (87 ± 10 μm vs 95 ± 8 μm; $p < 0.001$; Fig. 2). After compensation, pRNFL thickness remained significantly thinner in the MS participants as compared to controls (86 ± 9 μm vs 98 ± 7 μm; $p < 0.001$; Fig. 2). For macular layers, mRNFL (22 ± 3 μm vs 23 ± 3 μm; $p < 0.001$) and mGCL (46 ± 9 μm vs 54 ± 5 μm; $p = 0.026$) were significantly thinner in the MS participants (Fig. 2). There were no statistical differences in the retinal vessel density (MS: 3.68 ± 0.51 vs 3.77 ± 0.54; $p = 0.283$) and mIPL (MS: 38 ± 3 μm vs 38 ± 3 μm; $p = 0.403$) between groups.

We next examined the capability of the pRNFL, and the macular layers to differentiate MS participants from controls (Table 2). When mRNFL, mGCL, and mIPL measurements were combined (mGCC, AUC

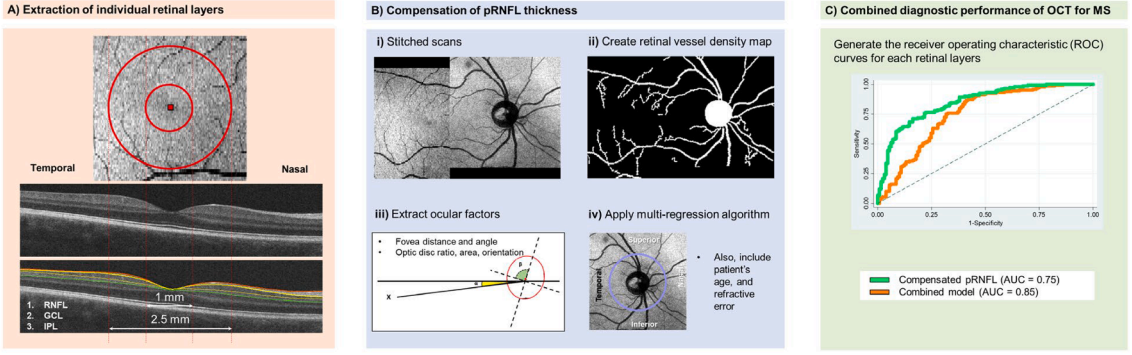

Fig. 1. Framework on the A) extraction of individual retinal layers at the macular region, namely the retinal nerve fibre layer (RNFL), ganglion cell layer (GCL), and inner plexiform layer (IPL) and the B) compensation of peripapillary RNFL (pRNFL). C) We then generated the receiver operating characteristic (ROC) curves for each retinal layer separately and combined the pRNFL retinal thickness with macular layers and compared the area under the curve (AUC) among the different models.

Table 1
Demographics and ocular characteristics of multiple sclerosis and healthy controls.

Characteristics	Healthy controls (n = 84 participants, 149 eyes)	Multiple sclerosis (n = 74 participants, 129 eyes)	P value
Age	39 ± 12	42 ± 11	0.128
Gender, female	54, 64%	49, 66%	0.799
Diabetes, no	84, 100%	74, 100%	–
Hypertension, no	74, 88%	71, 96%	0.087
Visual acuity, logMAR value (Snellen)	0.01 ± 0.02 (6/6^{-1})	0.01 ± 0.03 (6/6^{-1})	0.160
Intraocular pressure, mmHg	15.40 ± 2.60	17.57 ± 2.96	**<0.001**
Signal strength, peripapillary	8.49 ± 0.90	8.63 ± 0.92	0.207
Signal strength, macular	9.07 ± 0.91	9.22 ± 1.03	0.196
Optic disc area, mm^2	1.83 ± 0.33	1.82 ± 0.27	0.710
Optic disc ratio	1.10 ± 0.05	1.10 ± 0.06	0.433
Optic disc orientation, degrees	103.14 ± 28.78	98.93 ± 27.91	0.219
Fovea distance, μm	4.45 ± 0.24	4.49 ± 0.26	0.224
Fovea angle, degrees	−6.73 ± 2.96	−7.12 ± 3.40	0.310
Refractive error, dioptres	−0.14 ± 2.00	0.07 ± 1.35	0.319

Data presented are mean (SD) or number (%), as appropriate.
P value was obtained with independent *t*-test or Kruskal-Wallis for the continuous variables and with chi-square or Fisher's exact tests for categorical variables.

Table 2
Diagnostic performance for discriminating multiple sclerosis from healthy controls.

Model no:	Retinal Parameter	Area under the Receiver Operating Characteristic Curve (95% Confidence Interval)	Sensitivity at 80% Specificity	Best Cutoff (μm)	P value
1	Measured pRNFL thickness	0.75 (0.69–0.81)	47.7	97.0	Ref
2	Compensated pRNFL thickness	0.80 (0.75–0.85)	62.4	98.4	**0.020**
3	mGCIPL	0.74 (0.68–0.80)	46.3	92.1	0.612
4	mGCC	0.76 (0.70–0.81)	52.4	115.7	0.952
6	Combined (#2 and #4)	0.85 (0.80–0.89)	71.8	–	**<0.001**
7	Combined (#1 and #4)	0.82 (0.78–0.87)	67.1	–	**0.001**

Results for sensitivity is expressed as percentages; best cutoff is expressed in micrometers. P value indicates the paired comparisons with the best parameter (reference group).
pRNFL = peripapillary retinal nerve fiber layer; mGCIPL = macular ganglion cell layer plus inner plexiform layer; mGCC = macular ganglion cell complex (combined macular retinal nerve fiber layer, ganglion cell layer and inner plexiform layer).

= 0.76, p = 0.952 and mGCL plus mIPL [mGCIPL, AUC = 0.74, p = 0.612]), there was no significant difference as compared to measured pRNFL for MS differentiation (AUC, 0.75). Compensated pRNFL (AUC, 0.80) achieved better MS discrimination than measured pRNFL (AUC, 0.75; p = 0.020) and mGCIPL (AUC, 0.74; p = 0.025) but was statistically similar when compared to mGCC (AUC, 0.76; p = 0.057).

We also determine if combining optic disc with macular scans can improve OCT model performance for MS detection. Combining mGCC *plus* compensated pRNFL (AUC, 0.85) outperformed measured pRNFL (AUC, 0.75; p < 0.001; Table 2 **and** Fig. 3) as well as compensated pRNFL (AUC, 0.80; p = 0.007) for MS discrimination. The combination with mGCIPL similarly improved the AUC for differentiation of MS (AUC = 0.83 vs 0.75; p < 0.001; results not shown). The capability of OCT worsened slightly when we combined mGCC *plus* measured pRNFL as compared to the combined model with the compensating algorithm (AUC = 0.82 vs 0.85; p = 0.043; Table 2).

With specificity at 80% (or 20% false positive rate), 71.8% of MS participants were found to show abnormal results with macular (115.7 μm for mGCC) and peripapillary parameters (98.4 μm for compensated pRNFL thickness; Table 2).

The model improved the detection of recently diagnosed MS individuals from controls that agreed with our previous finding. Compensated pRNFL achieved slightly better performance than measured pRNFL for differentiation of recently diagnosed MS from controls (AUC, 0.70 vs 0.76; p = 0.048; Table 3). Combining macular and compensated pRNFL parameters provided the best discrimination of MS participants with disease duration of < 9 years (AUC = 0.87 vs 0.70; p < 0.001; Table 3). The finding was, however, different for those with disease duration of 9 years or longer. There was no difference in the

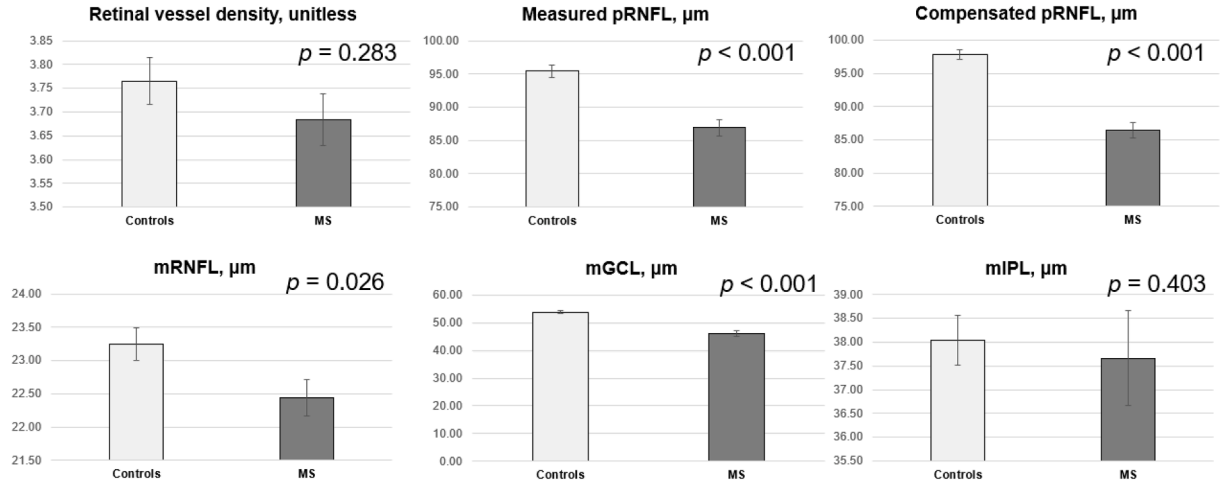

Fig. 2. Bar graphs showing the distribution of retinal vessel density, measured peripapillary retinal nerve fibre layer (pRNFL), compensated pRNFL, inner macular layers (mRNFL, ganglion cell layer [mGCL] and inner plexiform layer [mIPL]) between multiple sclerosis (MS) and controls. Data and P values shown are after adjustment for age, sex, hypertension, IOP, signal strength, and inter-eye correlation.

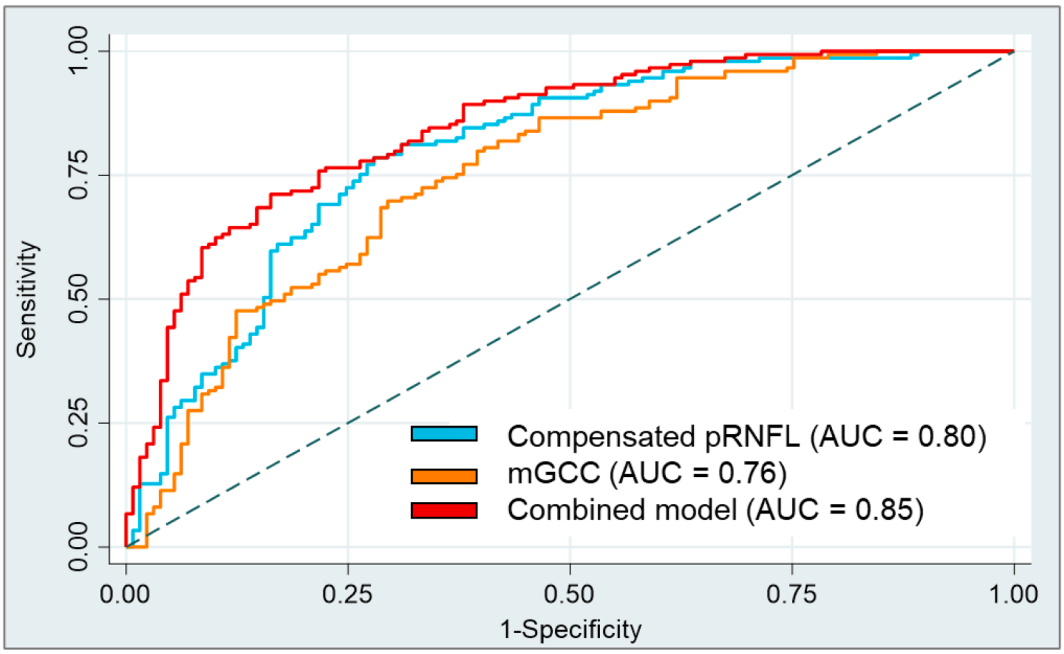

Fig. 3. Areas under the curve (AUC) of peripapillary retinal nerve fibre layer (pRNFL) thickness, macular ganglion cell complex (mGCC), and combined model (compensated pRNFL thickness, and mGCC) to discriminate multiple sclerosis (MS) and controls. mGCC represents RNFL, ganglion cell layer (GCL), and inner plexiform layer (IPL). There is an improvement in capability to distinguish MS from controls when the 2 best OCT parameters were combined (AUC = 0.85).

novel approach as compared to traditional OCT method to differentiate MS participants with long disease duration from controls.

We did not find any significant associations between OCT parameters and duration of MS or number of episodes (Table 4). Lower mGCIPL and mGCC thicknesses on OCT were independently associated with worse EDSS scores in MS (Table 4). Both measured ($p = 0.356$) and compensated cpRNFL ($p = 0.059$) were not associated with EDSS scores.

Because retinal asymmetry may contribute to the diagnosis of MS, we did a separate analysis only on participants with both eye data. We removed persons with single eye data (n = 38 eyes) which left us with 65 controls and 55 MS participants (Supplementary Table 1). The diagnostic performance to separate MS from controls was the best using mGCIPL (AUC = 0.75), followed by pRNFL (AUC = 0.71) whereas both intereye difference of mGCIPL (AUC = 0.44) and pRNFL (AUC = 0.39) performed poorly.

pRNFL thickness did not differ by the disease-modifying therapies (p = 0.172; Supplementary Table 2: glatiramer acetate (n = 31), subcutaneous interferon-β-1a (n = 9), intramuscular interferon-β-1a (n = 9), interferon-β-1b (n = 9), natalizumab (n = 7), teriflunomide (n = 7), and others (n = 2).

Table 3
Diagnostic performance for discriminating multiple sclerosis from healthy controls.

		Short duration (1–8 years; n = 40)		Long duration (9–37 years; n = 34)	
Model no:	Retinal Parameter	Area under the Receiver Operating Characteristic Curve (95% Confidence Interval)	P value	Area under the Receiver Operating Characteristic Curve (95% Confidence Interval)	P value
1	Measured pRNFL thickness	0.70 (0.62–0.79)	Ref	0.82 (0.76–0.89)	Ref
2	Compensated pRNFL thickness	0.76 (0.69–0.83)	**0.048**	0.86 (0.81–0.91)	0.109
3	mGCIPL	0.71 (0.63–0.78)	0.899	0.80 (0.73–0.88)	0.563
4	mGCC	0.70 (0.62–0.78)	0.960	0.83 (0.77–0.89)	0.826
6	Combined (#2 and #4)	0.87 (0.82–0.92)	**<0.001**	0.83 (0.77–0.89)	0.256

Results for sensitivity is expressed as percentages. P value indicates the paired comparisons with the best parameter (reference group).
pRNFL = peripapillary retinal nerve fiber layer; mGCIPL = macular ganglion cell layer plus inner plexiform layer; mGCC = macular ganglion cell complex (combined macular retinal nerve fiber layer, ganglion cell layer and inner plexiform layer).

4. Discussion

In this cross-sectional study, we improved the diagnostic accuracy of OCT to distinguish patients with relapsing-remitting MS with no optic neuritis from healthy controls by compensating pRNFL thickness measurements for ocular anatomical features. Of importance, the combination of scans from both the optic disc and macular regions, namely the mGCC and compensated pRNFL measurement values provided the highest diagnostic capability for MS. The combined model achieved a significantly better capability than measured pRNFL, with area under the ROC curve of 0.85 *versus* 0.75, translating to an average improvement in sensitivity of 24 percent for differentiation of MS individuals. Our study adds to a rapidly emergent field of using OCT measurements as retinal biomarkers for MS, by demonstrating that accounting for the pRNFL thickness measurements for individual variations as well as integrating macular information, may improve the utility of OCT in MS. Precise and earlier diagnosis of MS is recognized as a significant priority because of the availability of disease-modifying therapies, which affects an estimated 2.8 million people worldwide (Petzold et al., 2017).

4.1. Compensation of pRNFL for multiple factors improves the differentiation of MS

While some studies have shown a thinning in pRNFL thickness in MS patients without a history of optic neuritis (Albrecht et al., 2012; Gonzalez-Lopez et al., 2014; Para-Prieto et al., 2021; Parisi et al., 1999;

Table 4
Univariate analysis of optical coherence tomography parameters with duration of multiple sclerosis, number of episodes, and expanded disability status scale.

	Duration of multiple sclerosis			Numbers of episodes			EDSS		
Parameter	β	95% CI	*P* value*	β	95% CI	*P* value*	β	95% CI	*P* value*
Measured pRNFL thickness	−0.03	−0.06 to 0.01	0.120	−0.02	−0.05 to 0.04	0.949	−0.22	−0.68 to 0.24	0.356
Compensated pRNFL thickness	−0.04	−0.08 to 0.01	0.090	−0.01	−0.06 to 0.04	0.620	−0.33	−0.88 to 0.01	0.059
mGCIPL	−0.04	−0.08 to 0.01	0.088	−0.02	−0.06 to 0.02	0.322	−0.52	−0.94 to −0.10	**0.014**
mGCC	−0.04	−0.09 to 0.01	0.055	−0.03	−0.07 to 0.01	0.181	−0.46	−0.89 to −0.03	**0.036**

EDSS = expanded disability status scale; pRNFL = peripapillary retinal nerve fiber layer; mGCIPL = macular ganglion cell layer plus inner plexiform layer; mGCC = macular ganglion cell complex (combined macular retinal nerve fiber layer, ganglion cell layer and inner plexiform layer).

Syc et al., 2012), others have not found a significant difference between MS patients and controls (Behbehani et al., 2016; Knier et al., 2016; Oberwahrenbrock et al., 2013). Most of these studies have adjusted for the age when comparing the pRNFL measurements between MS and controls. Apart from age (Chua et al., 2020a), the pRNFL thickness measurement is influenced by individual ocular factors, such as axial length or refractive error, optic disc characteristics (size and area), disc-fovea angle, and retinal vessel profile (Budenz et al., 2007; Choi et al., 2014; Hood et al., 2008; Jonas et al., 2015; Resch et al., 2016). Patients with MS, particularly those with subclinical eye disease (unaffected by optic neuritis), may have miniscule retinal structural changes that may be confounded by the wide variability of pRNFL. Our compensation model comprises precise alignment of individual scans, adjustments of patient's anatomical features before comparison (Fig. 1**B**). As shown, our proposed compensated pRNFL resulted in an improvement in the diagnostic separation of MS from controls as compared to the traditional analysis of pRNFL. Routine clinical application of current advanced imaging analysis could be complex. Future studies should explore a time-efficient approach to optimize protocols such as combining peripapillary and macular information into a single index (Mwanza et al., 2018) and automating the OCT raw data compensation process.

The cohort of MS patients enrolled in the present study shows high variability in terms of disease duration. We further assessed the performance of the model in MS participants with short disease duration and long disease duration. We found that the combined model with the compensation approaches has value for MS detection in individuals with short disease duration but not for those with long disease duration. This implies that the compensating algorithms could represent a promising approach to improve OCT diagnostic accuracy in MS, but further studies enrolling a homogeneous cohort of early diagnosed MS patients or even clinically isolated syndrome (CIS) patients are needed to confirm this potentiality.

Future studies looking at longitudinal changes in MS will benefit from compensated pRNFL. We reported previously that the age-dependent thinning of pRNFL thickness was primarily due to the narrowing of retinal vessels instead of the loss of retinal ganglion cell axons (Chua et al., 2020a). Since current clinical OCT systems are as yet unable to separate retinal vessels from neuronal axons, conventional pRNFL measurements include retinal vessels. Therefore, the age-related narrowing of retinal vessels should be adjusted for when using pRNFL thickness measures over time.

4.2. Segmentation of individual retinal layers in MS

We segmented the individual layers of the inner macula with an automated open-source retinal segmentation algorithm (Abramoff et al., 2010). The software demonstrated high accuracy (Garvin et al., 2009) and reproducibility (Terry et al., 2016) in normal participants as well as patients with diabetic eye conditions. We found that eyes from patients with MS had significantly thinner mRNFL when compared to controls which is in good agreement with previous studies (Balk et al., 2014; Fernandes et al., 2013; Hokazono et al., 2013; Knier et al., 2016; Walter et al., 2012). Of note, macular GCL was statistically thinner in MS whereas there was no difference in the IPL between MS and controls. Although studies have reported a significant thinning of mGCIPL in non-optic neuritis eyes of MS patients, the mGCIPL incorporates not only the thickness of the ganglion cell layer but also that of the inner plexiform layer (Petzold et al., 2017). The result of our work further confirms the histopathologic study of postmortem MS eyes where they have identified retinal atrophy of the RNFL and GCL (Green et al., 2010). One potential reason why we did not see a difference in the IPL in MS may be because the IPL does not only contain dendrites of ganglion cells but also of other retinal cell types such as amacrine cells and bipolar cells (Zhang et al., 2021).

Our results indicate that mGCC improved the differentiation of MS from healthy controls more than mGCIPL. Since mGCC combined all 3 retinal layers (mRNFL, mGCL, and mIPL) whereas the mGCIPL included only 2 retinal layers, the inclusion of mRNFL in mGCC may improve the MS differentiation. As seen from Fig. 2, both mRNFL and mGCL were significantly thinner in the MS participants whereas there mIPL was statistically similar between groups. MS is a dynamic inflammatory disease, in which the optic nerve may swell subclincally and affect RNFL measures, while this does not happen so much with the GCL/GCIPL (Petzold et al., 2017).

4.3. Comparison of optic disc and macular scans to detect MS

From models 6 and 7, readers will be able to appreciate that the combination of disc and macular scans (without compensation) can improve MS detection as compared to using disc scan alone (AUC = 0.82 vs 0.75; $p = 0.001$). A previous study reported a lower diagnostic value of the optic disc pRNFL than the macular mGCC or mGCIPL imaging in MS (Garcia-Martin et al., 2014). The lower diagnostic ability of optic disc measurements is not expected as pRNFL analysis samples the axons from the entire retina. In contrast, macular analysis is based on the sampling of only 50% of the retinal ganglion cells' population and should technically be inferior in detecting retinal ganglion cell changes in MS (Na et al., 2011). This finding may be related to the variability among individuals in the characteristics of the optic disc such as the optic disc size and position of the optic disc relative to the macula whereas the macula is a relatively consistent structure between individuals. Also, pRNFL measurements are more affected by non-neural structures, such as blood vessels compared to macular measurements and, therefore, may be more susceptible to measurement variability (Hood et al., 2008).

Recent studies have shown intereye difference for pRNFL and mGCIPL can contribute to identifying unilateral optic nerve lesions and this may represent supportive measures for MS diagnosis (Nolan et al., 2018; Petzold et al., 2021). However, in the current study, the inter-eye absolute difference of pRNFL and mGCC did not improve the detection of MS from healthy controls as compared to the conventional approach. The limited diagnostic accuracy of retinal asymmetry may be due to study designs (community sample vs clinical sample), patient profiles such as MS disease activity, or co-morbidities (Petzold et al., 2021).

5. Strengths and limitations

Strengths of this study include a well-phenotyped cohort of MS

individuals without a history of optic neuritis, who were diagnosed according to internationally accepted criteria. This supports the concept that retinal neuronal loss occurs in MS without any clinically manifest ocular disease and supports the use of OCT scans as a complementary diagnostic imaging biomarker for MS workup. Since optic neuritis is a presenting feature in up to 50% of people with MS, the exclusion of people with a history of ON in either eye may have biased the cohort. We intentionally excluded individuals with a history of optic neuritis in either eye as we wanted to assess if OCT could determine differentiate MS of a less inflammatory phenotype. In addition, a standardized study methodology was used for OCT analysis that accounts for the variability of ocular anatomy and angioarchitecture in individuals that can be easily applied to OCT scans from different vendors and is fully automated. Furthermore, we statistically adjusted for potential confounders of retinal thickness measurements such as age, sex, systemic hypertension, IOP, and signal strength. We also performed OCT magnification correction using axial length measurements to ensure the accuracy of the retinal thickness measurements.

A potential limitation of the study includes the small sample size which reduces the generalizability of the study. In addition, only one OCT device was tested, limiting the results to the Cirrus device. Another potential limitation is that macular data is not compensated whereas optic nerve data is. As discussed earlier, uncompensated macular data should not affect the results much due to the more consistent measurements of the macula. Another limitation of the study is the lack of MRI data to study the relation of brain atrophy measures with the novel OCT measures. It must be stated, however, that none of the parameters correlated with disease duration or the number of neurologic episodes. Longitudinal studies are required to investigate whether thinning of retinal layers is related to the occurrence of neurologic episodes. There is a potential concern that some of the MS participants may have glaucoma as their IOP levels were significantly higher than normal controls. We ruled out the presence of glaucomatous optic neuropathy via an ophthalmological examination. Even though our MS patients had statistically higher IOP than controls (17.57 $\pm$ 2.96), the IOP level was similar to the control group of a previous paper (17 mmHg) (Lincoff et al., 2017).

6. Conclusion

In summary, our study showed that the diagnostic accuracy of the OCT to distinguish relapsing-remitting MS from controls can be improved, by compensating the pRNFL thickness measurements for individual differences and combining macular information. Our study clearly shows that axonal thinning is a feature independent of optic neuritis in MS and that the mGCC is a valuable complementary diagnostic tool to pRNFL analysis. The improvements in the diagnostic accuracy for MS detection should assist to improve the potential application of OCT on MS diagnostics, where axonal degeneration and neuronal loss in MS patients are monitored and used as biomarkers. At present, diagnostic implications of OCT used for MS detection should be interpreted with care. Although on a group level the present study and previous literature (Petzold et al., 2017) demonstrated clear differences in terms of retinal parameters between MS patients and healthy controls, OCT results from a single individual often does not allow a sharp distinction between the two conditions. This aspect is particularly relevant in early MS patients: on the one hand, the advantages deriving from OCT advanced analysis approaches are expected to be greater in this phase of the disease (as seen from results on those with a short disease duration of $<$9 years), on the other hand in the early phase of the disease the overlap with the general population is expected to be greater (especially in the case of a non-visual onset, a significant proportion of MS subjects would show normal standard OCT examination). Nevertheless, this kind of approach could promote in the near future OCT inclusion among routine MS diagnostic work-up, together with other paraclinical techniques.

Data availability

The data may be made available via a request to the Authors, on the condition of a formal data sharing agreement, submission of a formal project outline as well as a requirement for co-authorship.

CRediT authorship contribution statement

Jacqueline Chua: Conceptualization, Methodology, Formal analysis, Writing – review & editing, Project administration, Funding acquisition. **Mihai Bostan:** Conceptualization, Methodology, Investigation, Writing – original draft, Writing – review & editing, Project administration. **Chi Li:** Writing – review & editing, Project administration. **Yin Ci Sim:** Writing – review & editing, Project administration. **Inna Bujor:** Investigation, Writing – review & editing, Project administration. **Damon Wong:** Writing – review & editing, Project administration. **Bingyao Tan:** Writing – review & editing, Project administration. **Xinwen Yao:** Writing – review & editing, Project administration. **Florian Schwarzhans:** Writing – review & editing, Project administration. **Gerhard Garhöfer:** Writing – review & editing, Project administration, Project administration. **Georg Fischer:** Writing – review & editing, Project administration. **Clemens Vass:** . **Cristina Tiu:** Writing – review & editing, Project administration. **Ruxandra Pirvulescu:** Investigation, Writing – review & editing, Project administration. **Alina Popa-Cherecheanu:** Conceptualization, Methodology, Investigation, Writing – review & editing, Project administration. **Leopold Schmetterer:** Conceptualization, Methodology, Writing – original draft, Writing – review & editing, Project administration, Supervision, Funding acquisition.

Declaration of Competing Interest

The authors declare that they have no known competing financial interests or personal relationships that could have appeared to influence the work reported in this paper.

Acknowledgements

Ms. Hexuan Tang, made substantial contributions to the data quality assessment of the optical coherence tomography scans, and macular layer segmentation.

Funding

This work was funded by grants from the National Medical Research Council (CG/C010A/2017_SERI; OFIRG/0048/2017; OFLCG/004c/2018; TA/MOH-000249-00/2018 MOH-OFIRG20nov-0014 and NMRC/CG2/004b/2022-SERI), National Research Foundation Singapore (NRF2019-THE002-0006 and NRF-CRP24-2020-0001), A*STAR (A20H4b0141), the Singapore Eye Research Institute & Nanyang Technological University (SERI-NTU Advanced Ocular Engineering (STANCE) Program), the Duke-NUS Medical School (Duke-NUS-KP (Coll)/2018/0009A), and the SERI-Lee Foundation (LF1019-1) Singapore.

Appendix A. Supplementary data

Supplementary data to this article can be found online at https://doi.org/10.1016/j.nicl.2022.103010.

References

Abramoff, M.D., Garvin, M.K., Sonka, M., 2010. Retinal imaging and image analysis. IEEE Rev. Biomed. Eng. 3, 169–208.

Albrecht, P., Ringelstein, M., Müller, A.K., Keser, N., Dietlein, T., Lappas, A., Foerster, A., Hartung, H.P., Aktas, O., Methner, A., 2012. Degeneration of retinal layers in

multiple sclerosis subtypes quantified by optical coherence tomography. Mult. Scler. 18 (10), 1422–1429.
Aytulun, A., Cruz-Herranz, A., Aktas, O., Balcer, L.J., Balk, L., Barboni, P., Blanco, A.A., Calabresi, P.A., Costello, F., Sanchez-Dalmau, B., DeBuc, D.C., Feltgen, N., Finger, R. P., Frederiksen, J.L., Frohman, E., Frohman, T., Garway-Heath, D., Gabilondo, I., Graves, J.S., Green, A.J., Hartung, H.-P., Havla, J., Holz, F.G., Imitola, J., Kenney, R., Klistorner, A., Knier, B., Korn, T., Kolbe, S., Krämer, J., Lagrèze, W.A., Leocani, L., Maier, O., Martínez-Lapiscina, E.H., Meuth, S., Outteryck, O., Paul, F., Petzold, A., Pihl-Jensen, G., Preiningerova, J.L., Rebolleda, G., Ringelstein, M., Saidha, S., Schippling, S., Schuman, J.S., Sergott, R.C., Toosy, A., Villoslada, P., Wolf, S., Yeh, E. A., Yu-Wai-Man, P., Zimmermann, H.G., Brandt, A.U., Albrecht, P., 2021. APOSTEL 2.0 recommendations for reporting quantitative optical coherence tomography studies. Neurology 97 (2), 68–79.
Balk, L.J., Twisk, J.W.R., Steenwijk, M.D., Daams, M., Tewarie, P., Killestein, J., Uitdehaag, B.M.J., Polman, C.H., Petzold, A., 2014. A dam for retrograde axonal degeneration in multiple sclerosis? J. Neurol. Neurosurg. Psychiatry 85 (7), 782–789.
Behbehani, R., Al-Moosa, A., Sriraman, D., Alroughani, R., 2016. Ganglion cell analysis in acute optic neuritis. Mult. Scler. Relat. Disord. 5, 66–69.
Bennett, A.G., Rudnicka, A.R., Edgar, D.F., 1994. Improvements on Littmann's method of determining the size of retinal features by fundus photography. Graefes Arch. Clin. Exp. Ophthalmol. 232 (6), 361–367.
Budenz, D.L., Anderson, D.R., Varma, R., Schuman, J., Cantor, L., Savell, J., Greenfield, D.S., Patella, V.M., Quigley, H.A., Tielsch, J., 2007. Determinants of normal retinal nerve fiber layer thickness measured by Stratus OCT. Ophthalmology 114 (6), 1046–1052.
Button, J., Al-Louzi, O., Lang, A., Bhargava, P., Newsome, S.D., Frohman, T., Balcer, L.J., Frohman, E.M., Prince, J., Calabresi, P.A., Saidha, S., 2017. Disease-modifying therapies modulate retinal atrophy in multiple sclerosis: a retrospective study. Neurology 88 (6), 525–532.
Choi, J.A., Kim, J.S., Park, H.Y., Park, H., Park, C.K., 2014. The foveal position relative to the optic disc and the retinal nerve fiber layer thickness profile in myopia. Invest. Ophthalmol. Vis. Sci. 55, 1419–1426.
Chua, J., Schwarzhans, F., Nguyen, D.Q., Tham, Y.C., Sia, J.T., Lim, C., Mathijia, S., Cheung, C., Tin, A., Fischer, G., Cheng, C.-Y., Vass, C., Schmetterer, L., 2020a. Compensation of retinal nerve fibre layer thickness as assessed using optical coherence tomography based on anatomical confounders. Br. J. Ophthalmol. 104 (2), 282–290.
Chua, J., Tan, B., Ke, M., Schwarzhans, F., Vass, C., Wong, D., Nongpiur, M.E., Wei Chua, M.C., Yao, X., Cheng, C.-Y., Aung, T., Schmetterer, L., 2020b. Diagnostic ability of individual macular layers by spectral-domain OCT in different stages of glaucoma. Ophthalmol Glaucoma 3 (5), 314–326.
Cleves, M.A., 2002. From the help desk: comparing areas under receiver operating characteristic curves from two or more probit or logit models. Stata J. 2 (3), 301–313.
Fernandes, D.B., Raza, A.S., Nogueira, R.G.F., Wang, D., Callegaro, D., Hood, D.C., Monteiro, M.L.R., 2013. Evaluation of inner retinal layers in patients with multiple sclerosis or neuromyelitis optica using optical coherence tomography. Ophthalmology 120 (2), 387–394.
Garcia-Martin, E.S., Rojas, B., Ramirez, A.I., de Hoz, R., Salazar, J.J., Yubero, R., Gil, P., Trivino, A., Ramirez, J.M., 2014. Macular thickness as a potential biomarker of mild Alzheimer's disease. Ophthalmology 121, 1149-1151 e1143.
Garvin, M.K., Abramoff, M.D., Wu, X., Russell, S.R., Burns, T.L., Sonka, M., 2009. Automated 3-D intraretinal layer segmentation of macular spectral-domain optical coherence tomography images. IEEE Trans. Med. Imaging 28, 1436–1447.
Gonzalez-Lopez, J.J., Rebolleda, G., Leal, M., Oblanca, N., Munoz-Negrete, F.J., Costa-Frossard, L., Alvarez-Cermeno, J.C., 2014. Comparative diagnostic accuracy of ganglion cell-inner plexiform and retinal nerve fiber layer thickness measures by Cirrus and Spectralis optical coherence tomography in relapsing-remitting multiple sclerosis. Biomed Res. Int. 2014, 128517.
Green, A.J., McQuaid, S., Hauser, S.L., Allen, I.V., Lyness, R., 2010. Ocular pathology in multiple sclerosis: retinal atrophy and inflammation irrespective of disease duration. Brain 133 (6), 1591–1601.
Hanley, J.A., McNeil, B.J., 1983. A method of comparing the areas under receiver operating characteristic curves derived from the same cases. Radiology 148 (3), 839–843.
Higashide, T., Ohkubo, S., Hangai, M., Ito, Y., Shimada, N., Ohno-Matsui, K., Terasaki, H., Sugiyama, K., Chew, P., Li, K.K., Yoshimura, N., 2016. Influence of clinical factors and magnification correction on normal thickness profiles of macular retinal layers using optical coherence tomography. PLoS One 11, e0147782.
Hokazono, K., Raza, A.S., Oyamada, M.K., Hood, D.C., Monteiro, M.L.R., 2013. Pattern electroretinogram in neuromyelitis optica and multiple sclerosis with or without optic neuritis and its correlation with FD-OCT and perimetry. Doc. Ophthalmol. 127 (3), 201–215.
Hood, D.C., Fortune, B., Arthur, S.N., Xing, D., Salant, J.A., Ritch, R., Liebmann, J.M., 2008. Blood vessel contributions to retinal nerve fiber layer thickness profiles measured with optical coherence tomography. J. Glaucoma 17, 519–528.
Jonas, R.A., Wang, Y.X., Yang, H., Li, J.J., Xu, L., Panda-Jonas, S., Jonas, J.B., 2015. Optic Disc - Fovea Angle: the Beijing eye study 2011. PLoS One 10, e0141771.
Knier, B., Berthele, A., Buck, D., Schmidt, P., Zimmer, C., Mühlau, M., Hemmer, B., Korn, T., 2016. Optical coherence tomography indicates disease activity prior to clinical onset of central nervous system demyelination. Mult. Scler. 22 (7), 893–900.
Kurtzke, J.F., 1983. Rating neurologic impairment in multiple sclerosis: an expanded disability status scale (EDSS). Neurology 33, 1444–1452.
Leung, C.K., Cheng, A.C., Chong, K.K., Leung, K.S., Mohamed, S., Lau, C.S., Cheung, C.Y., Chu, G.C., Lai, R.Y., Pang, C.C., Lam, D.S., 2007. Optic disc measurements in myopia with optical coherence tomography and confocal scanning laser ophthalmoscopy. Invest. Ophthalmol. Vis. Sci. 48, 3178–3183.
Lincoff, N.S., Buccilli, A., Weinstock-Guttman, B., Sieminski, S., Gandhi, S., 2017. Is multiple sclerosis associated with a lower intraocular pressure? J. Neuroophthalmol. 37, 265–267.
McGinley, M.P., Goldschmidt, C.H., Rae-Grant, A.D., 2021. Diagnosis and treatment of multiple sclerosis: a review. JAMA 325, 765–779.
Mwanza, J.C., Warren, J.L., Budenz, D.L., 2018. Utility of combining spectral domain optical coherence tomography structural parameters for the diagnosis of early Glaucoma: a mini-review. Eye Vis. (Lond) 5, 9.
Na, J.H., Sung, K.R., Baek, S., Sun, J.H., Lee, Y., 2011. Macular and retinal nerve fiber layer thickness: which is more helpful in the diagnosis of glaucoma? Invest. Ophthalmol. Vis. Sci. 52, 8094–8101.
Nolan, R.C., Galetta, S.L., Frohman, T.C., Frohman, E.M., Calabresi, P.A., Castrillo-Viguera, C., Cadavid, D., Balcer, L.J., 2018. Optimal intereye difference thresholds in retinal nerve fiber layer thickness for predicting a unilateral optic nerve lesion in multiple sclerosis. J. Neuroophthalmol. 38, 451–458.
Oberwahrenbrock, T., Ringelstein, M., Jentschke, S., Deuschle, K., Klumbies, K., Bellmann-Strobl, J., Harmel, J., Ruprecht, K., Schippling, S., Hartung, H.-P., Aktas, O., Brandt, A.U., Paul, F., 2013. Retinal ganglion cell and inner plexiform layer thinning in clinically isolated syndrome. Mult. Scler. 19 (14), 1887–1895.
Para-Prieto, M., Martin, R., Crespo, S., Mena-Garcia, L., Valisena, A., Cordero, L., Gonzalez Fernandez, G., Arenillas, J.F., Tellez, N., Pastor, J.C., 2021. OCT variability prevents their use as robust biomarkers in multiple sclerosis. Clin. Ophthalmol. 15, 2025–2036.
Parisi, V., Manni, G., Spadaro, M., Colacino, G., Restuccia, R., Marchi, S., Bucci, M.G., Pierelli, F., 1999. Correlation between morphological and functional retinal impairment in multiple sclerosis patients. Invest. Ophthalmol. Vis. Sci. 40, 2520–2527.
Pereira, I., Resch, H., Schwarzhans, F., Wu, J., Holzer, S., Kiss, B., Frommlet, F., Fischer, G., Vass, C., 2015. Multivariate model of the intersubject variability of the retinal nerve fiber layer thickness in healthy subjects. Invest. Ophthalmol. Vis. Sci. 56, 5290–5298.
Pereira, I., Weber, S., Holzer, S., Resch, H., Kiss, B., Fischer, G., Vass, C., 2014. Correlation between retinal vessel density profile and circumpapillary RNFL thickness measured with Fourier-domain optical coherence tomography. Br. J. Ophthalmol. 98 (4), 538–543.
Petzold, A., Balcer, L.J., Calabresi, P.A., Costello, F., Frohman, T.C., Frohman, E.M., Martinez-Lapiscina, E.H., Green, A.J., Kardon, R., Outteryck, O., Paul, F., Schippling, S., Vermersch, P., Villoslada, P., Balk, L.J., Ern-Eye, I., 2017. Retinal layer segmentation in multiple sclerosis: a systematic review and meta-analysis. Lancet Neurol. 16, 797–812.
Petzold, A., Chua, S.Y.L., Khawaja, A.P., Keane, P.A., Khaw, P.T., Reisman, C., Dhillon, B., Strouthidis, N.G., Foster, P.J., Patel, P.J., Eye, U.K.B., Vision, C., 2021. Retinal asymmetry in multiple sclerosis. Brain 144, 224–235.
Resch, H., Pereira, I., Hienert, J., Weber, S., Holzer, S., Kiss, B., Fischer, G., Vass, C., 2016. Influence of disc-fovea angle and retinal blood vessels on interindividual variability of circumpapillary retinal nerve fibre layer. Br. J. Ophthalmol. 100 (4), 531–536.
Savini, G., Barboni, P., Parisi, V., Carbonelli, M., 2012. The influence of axial length on retinal nerve fibre layer thickness and optic-disc size measurements by spectral-domain OCT. Br. J. Ophthalmol. 96 (1), 57–61.
Syc, S.B., Saidha, S., Newsome, S.D., Ratchford, J.N., Levy, M., Ford, E., Crainiceanu, C. M., Durbin, M.K., Oakley, J.D., Meyer, S.A., Frohman, E.M., Calabresi, P.A., 2012. Optical coherence tomography segmentation reveals ganglion cell layer pathology after optic neuritis. Brain 135, 521–533.
Terry, L., Cassels, N., Lu, K., Acton, J.H., Margrain, T.H., North, R.V., Fergusson, J., White, N., Wood, A., 2016. Automated retinal layer segmentation using spectral domain optical coherence tomography: evaluation of inter-session repeatability and agreement between devices. PLoS One 11, e0162001.
Tewarie, P., Balk, L., Costello, F., Green, A., Martin, R., Schippling, S., Petzold, A., 2012. The OSCAR-IB consensus criteria for retinal OCT quality assessment. PLoS One 7, e34823.
Thompson, A.J., Banwell, B.L., Barkhof, F., Carroll, W.M., Coetzee, T., Comi, G., Correale, J., Fazekas, F., Filippi, M., Freedman, M.S., Fujihara, K., Galetta, S.L., Hartung, H.P., Kappos, L., Lublin, F.D., Marrie, R.A., Miller, A.E., Miller, D.H., Montalban, X., Mowry, E.M., Sorensen, P.S., Tintore, M., Traboulsee, A.L., Trojano, M., Uitdehaag, B.M.J., Vukusic, S., Waubant, E., Weinshenker, B.G., Reingold, S.C., Cohen, J.A., 2018. Diagnosis of multiple sclerosis: 2017 revisions of the McDonald criteria. Lancet Neurol. 17, 162–173.
Walter, S.D., Ishikawa, H., Galetta, K.M., Sakai, R.E., Feller, D.J., Henderson, S.B., Wilson, J.A., Maguire, M.G., Galetta, S.L., Frohman, E., Calabresi, P.A., Schuman, J. S., Balcer, L.J., 2012. Ganglion cell loss in relation to visual disability in multiple sclerosis. Ophthalmology 119, 1250–1257.
Zhang, T., Kho, A.M., Srinivasan, V.J., 2021. In vivo morphometry of inner plexiform layer (IPL) stratification in the human retina with visible light optical coherence tomography. Front. Cell. Neurosci. 15, 655096.